AD-A148 854

LCPL

AD A148854

BRL

TECHNICAL REPORT BRL-TR-2602

EFFECTS OF PERFORATION L/D RATIO AND SLOTTING ON STICK PROPELLANT COMBUSTION

Arpad A. Juhasz
Frederick W. Robbins
Roger E. Bowman
J. Omar Doali
William P. Aungst

October 1984

US ARMY BALLISTIC RESEARCH LABORATORY
ABERDEEN PROVING GROUND, MARYLAND

UNCLASSIFIED

SECURITY CLASSIFICATION OF THIS PAGE (When Data Entered)

REPORT DOCUMENTATION PAGE

READ INSTRUCTIONS BEFORE COMPLETING FORM

1. REPORT NUMBER: TECHNICAL REPORT BRL-TR-2602	2. GOVT ACCESSION NO.
3. RECIPIENT'S CATALOG NUMBER	
4. TITLE (and Subtitle): Effects of Perforation L/D Ratio and Slotting on Stick Propellant Combustion	5. TYPE OF REPORT & PERIOD COVERED: Final 1981-1983
	6. PERFORMING ORG. REPORT NUMBER
7. AUTHOR(s): Arpad A. Juhasz, Frederick W. Robbins, Roger E. Bowman, J. Omar Doali, William P. Aungst	8. CONTRACT OR GRANT NUMBER(s)
9. PERFORMING ORGANIZATION NAME AND ADDRESS: US Army Ballistic Research Laboratory, ATTN: AMXBR-IBD, Aberdeen Proving Ground, MD 21005-5066	10. PROGRAM ELEMENT, PROJECT, TASK AREA & WORK UNIT NUMBERS: 1L162618AH80
11. CONTROLLING OFFICE NAME AND ADDRESS: US Army Ballistic Research Laboratory, ATTN: AMXBR-OD-ST, Aberdeen Proving Ground, Md 21005-5066	12. REPORT DATE: October 1984
	13. NUMBER OF PAGES: 41
14. MONITORING AGENCY NAME & ADDRESS (if different from Controlling Office)	15. SECURITY CLASS. (of this report): Unclassified
	15a. DECLASSIFICATION/DOWNGRADING SCHEDULE

16. DISTRIBUTION STATEMENT (of this Report)

Approved for public release, distribution unlimited

17. DISTRIBUTION STATEMENT (of the abstract entered in Block 20, if different from Report)

18. SUPPLEMENTARY NOTES

19. KEY WORDS (Continue on reverse side if necessary and identify by block number)

20. ABSTRACT (Continue on reverse side if necessary and identify by block number)

Closed bomb combustion studies were performed on single-perforated (1P) and slotted 1P NOSOL 363 propellant samples ranging in length from 19 to 338 mm. Samples having equal webs, but differing in their perforation diameters as well as lengths were examined. Samples with larger perforation diameters (PD) (2.13 mm) showed an increase of observed burning rate with length. For example, at 200 MPa, the burning rate of the 338 mm samples was 17 percent greater than the burning rate of the 19 mm long samples. In the case of the

DD FORM 1 JAN 73 1473 EDITION OF 1 NOV 65 IS OBSOLETE

UNCLASSIFIED

SECURITY CLASSIFICATION OF THIS PAGE (When Data Entered)

20. Abstract (Cont'd):

samples with smaller (0.940 mm) perforation diameter, however, the fastest burning rates were observed for the medium length (168 mm) rather than the longest samples. All slotted and short granular propellant samples, irrespective of perforation diameter, exhibited essentially identical burning rate characteristics. The studies indicate that, at least under closed bomb conditions, slotted 1P stick propellants burn just like granular propellants. In the case of unslotted 1P stick propellants, however, complex burning augmentation effects exist. Some of the mechanisms may involve increases in the burning rate inside the perforations due to enhanced pressure and/or erosive burning effects as well as grain splitting. Modeling propellant burning via the grain splitting and pressure build up hypotheses was partially successful in accounting for the observed effects.

SUMMARY

Combustion properties of slotted and unslotted single perforated (1P) stick propellant samples were examined using closed bomb and interrupted burning techniques. All samples were prepared from a single lot of NOSOL 363 propellant. The maximum sample length studied was 337 mm. The results of the study indicate a significant difference in the burning characteristics of some of the slotted and unslotted samples. Whereas the burning rates of slotted stick propellants were found to be independent of grain length and perforation diameter, the burning rates of unslotted samples were found to be strongly affected by both parameters. (It seems reasonable to assume that these observations would also hold in a general way for propellants made using different chemistries.) The burning augmentation with grain length is not a simple relationship, however. Although burning rate increase was found to correlate with grain length for all the larger (2.13 mm) perforation diameter (PD) unslotted samples studied, the correlation did not hold true for the smaller (.940 mm) PD samples. In the case of the latter, the greatest burning rate augmentation was observed for the medium, rather than the longest samples. Overall, it appears that slotted 1P stick propellants burn according to Piobert's law irrespective of grain length, whereas unslotted 1P stick propellants do not.

Interrupted burning tests indicate that perforation-augmented burning, as evidenced by severe coning and greater regression within the perforation than the grain exterior, can take place. This was the case for the 143 mm long samples having a 0.940 mm perforation diameter. Appropriately, similar samples, when burned in a closed bomb, exhibited strongly enhanced burning rates. On the other hand, interrupted burning experiments with samples of identical length but a larger (2.13 mm) PD showed little evidence of augmented burning. Consistently, only a negligible increase in closed bomb burning rates was observed for samples in this length and perforation diameter range. These observations demonstrate that a perforation dependent augmentation of observed burning rates is possible. Further, the dependence appears to be a function of both perforation length and diameter.

Possible mechanisms for the observed augmentation include a simple pressure augmented burning in the perforation, erosive burning, and grain fracture. The pressure- and fracture-augmented hypotheses were examined numerically using IBHVG, a lumped parameter interior ballistic code and CBRED2, our normal closed bomb burning rate analysis program. Although no exact matching of the observed phenomena resulted, several consistent trends were noted. On the one hand, the degressive character of the burning rate curves from the fracture mechanism simulations was similar to that experimentally observed for the longest of the small-perforation samples. On the other hand, simulations assuming perforation pressure buildup also resulted in augmented burning rate curves. The order of augmentation was inverted, however. That is to say, whereas the computed predictions called for greater enhancement of the samples with small perforation diameters; in fact, the experimental results indicated greater enhancement for the samples with larger perforation diameters.

There is considerable independent evidence for grain fracture in unslotted 1P stick propellant burning under gun conditions. Stick propellants examined for use in advanced US artillery charges have generally been much

longer (and in the case of the M30A1 propellants, more brittle) than the samples used in this study. Due to size limitations on our bombs, sample lengths had to be greatly reduced. It is reasonable to assume that we would have observed more grain fracture had we been firing the full gun-length propellant samples. As it is, we feel that grain fracture was the controlling mechanism in the combustion of only the longest, small perforation diameter samples. From the results on the remaining samples, it appears that significant burning rate augmentation can take place without grain fracture. Mechanistically, it is likely that perforation pressure buildup, erosive burning, and grain fracture are stages in a natural progression. The relative importance of the stages in the burning of an actual propellant charge probably depends upon factors such as propellant energy, intrinsic burning rate, mechanical properties, and geometry (grain length, perforation diameter, and web).

TABLE OF CONTENTS

LIST OF ILLUSTRATIONS

I. INTRODUCTION

The use of bundles of propellant sticks in artillery charges offers many potential advantages both in simplifying charge construction as well as in improvements in interior ballistic performance. The natural flow channels between sticks provide a ready means for propagation of igniter gases into and the flow of combustion products out of the propelling charge. Recent experimental and theoretical efforts have demonstrated quite conclusively that the use of stick propellants can drastically reduce pressure waves, especially in the case of top zone charges in large caliber guns.[1,2,3,4] The pressure-wave reductions, in turn, can readily be translated into improvements in weapon safety and shot-to-shot reproducibility. There are further indications that stick propellant charges may function with higher thermodynamic efficiencies than granular charges.[5] This would lead to equivalent performance at lower charge weights. The use of stick propellants in future United States artillery systems seems assured provided that the practical problems relating to production and reproducibility can be successfully solved.

Stick propellants in various forms have been used in guns for close to a century. In fact, the British term "cordite" can be traced back to an early double-base propellant composition which was extruded as nonperforated cylinders (cords) cut to fit the length of the gun chamber. Subsequent developments in stick propellants introduced a perforation in the center of the stick to take advantage of the superior form function of the single perforated geometry. Anomalies were noted, however, in the burning of the perforated sticks. This lead to the introduction of a slot along the length of the stick to permit lateral venting of the combustion products from the perforation.[6] Slotted stick propellants appear to be well behaved and current

---

[1] *A. W. Horst and T. C. Minor, "Improved Flow Dynamics in Guns Through the Use of Alternative Propellant Geometries," 1980 JANNAF Propulsion Meeting, CPIA Publication 315, Vol I, pp 325-352, March 1980.*

[2] *T. C. Smith, "Experimental Gun Testing of High Density Multiperforated Stick Propellant Charge Assemblies," 17th JANNAF Combustion Meeting, CPIA Publication 329, Vol II, pp 87-96, November 1980.*

[3] *T. C. Smith and J. A. Kudzall, "Evaluation of Stick Propellant Charge Concepts," 16th JANNAF Combustion Meeting, CPIA Publication 308, Vol I, pp 417-432, December 1979.*

[4] *F. W. Robbins, J. A. Kudzall, J. A. McWilliams, and P. S. Gough, "Experimental Determination of Stick Charge Flow Resistance," 17th JANNAF Combustion Meeting, CPIA Publication 329, Vol II, pp 97-118, November 1980.*

[5] *S. Weiner, "Investigation of Stick Propellant for 155-mm Howitzer, XM198," Interim Memorandum Report, Picatinny Arsenal, July 1975.*

[6] *J. Corner, Theory of the Interior Ballistics of Guns, John Wiley and Sons, NY, 1950.*

European practice leans heavily in favor of the slotted configuration.[7,8] There is a feeling, however, that given an understanding of 1P stick propellant burning, certain progressive burning properties of the 1P stick propellants may be exploitable in future gun systems.

The BRL has recently been engaged in interior ballistic modeling of stick propellant charge performance. Normally interior ballistic simulations are made on the basis (inter alia) of propellant burning rate data obtained from closed bomb firings. For granular charges, agreement between experiment and prediction is generally excellent. Attempting this approach with stick propellant systems, however, resulted in serious differences between experimental and theoretical results.[8] Predicted maximum pressures were 10-25 percent low for unslotted 1P stick propellants, and 5-10 percent low for slotted 1P stick propellants. These results are not atypical of findings elsewhere.[9] Part of the difficulty probably stems from the fact that the closed bomb burning rates of the propellants (which can be as long as 710 mm in the gun) were obtained on samples cut to fit into the standard (350 mm long) 700 cm^3 closed bombs. In other cases, the burning rates used in the interior ballistic codes for stick charges were extrapolated from granular propellant burning rate data. Clearly, stick propellants seem to have some unusual burning characteristics in guns. The objective of this study was to examine, by means of the closed bomb, the variations of extracted burning rates as a function of grain length and the presence or absence of a slot along the length of the grain. The scope of the study included a variation of the perforation diameter and the mode of sample ignition. The results of the exercise were to be used in further interior ballistic modeling efforts for stick propellant systems.

II. EXPERIMENTAL DETAILS

A. Propellants

The propellant, NOSOL 436, Lot RAD 1-2 of 1973, was manufactured at Radford Army Ammunition Plant. Chemically, the composition is identical to NOSOL 363. This is a solventless modified double-base propellant manufactured in "carpet rolls." The material was subsequently extruded into single perforated sticks at the Naval Ordnance Station, Indian Head, Maryland. Slotted samples were prepared at the BRL using the device pictured in Figure 1. Dimensional information for the two sample types appears in Table I.

---

[7] *I. W. May and T. C. Minor, "European Trip Report, 18 June - 2 July 1979," Applied Ballistics Branch, Interior Ballistics Division (DRDAR-BLP), Ballistic Research Laboratory, Aberdeen Proving Ground, MD, 1 May 1980.*

[8] *F. W. Robbins and A. W. Horst, "A Single Theoretical Analysis and Experimental Investigation of Burning Processes of Stick Propellant," 18th JANNAF Combustion Meeting, CPIA Publication 347, Vol I, pp 25-34, October 1981.*

[9] *A. Grabowski, S. Weiner and A. J. Beardell, "Closed Bomb Testing of Stick Propellant in Gun Firing Simulation," 17th JANNAF Combustion Meeting, CPIA Publication 329, Vol II, pp 119-124, November 1980.*

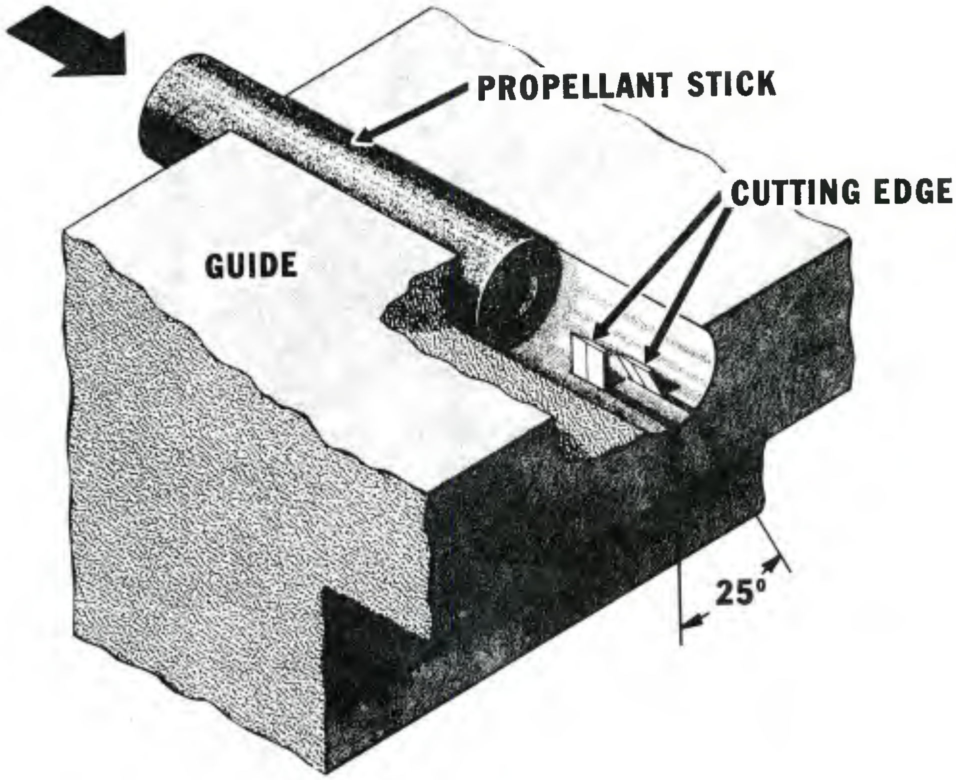

Figure 1. Device for Preparing Slotted Samples

TABLE I. DIMENSIONAL INFORMATION FOR NOSOL 363 TEST SAMPLES

Parameter	Propellant A	Propellant B
Outer Diameter (mm)	6.502	7.620
Inner Diameter (mm)	0.940	2.134
Web (mm)	2.794	2.743
Length (mm)	*	*
Slot Width (inner) (mm)	0.813	0.711
Slot Width (outer) (mm)	1.727	1.829

* Sample lengths varied from 19.05 to 336.6 mm. Specifics appear in Table II.

B. Test Matrix

Selection of samples, sample lengths, and choice of slotted versus uslotted 1P sample geometries was made to maximize (within limits of existing equipment) the probability of finding differences in extracted burning rates ascribable strictly to changes in propellant geometry. The sample matrix for the study is given in Table II. End views of various slotted and unslotted 1P samples appear in Figure 2. Sample lengths varied from 19 to 337 mm giving a range of perforation length to diameter ratios from 9 to 358.

C. Interrupted Burning Experiments

Interrupted burning experiments were performed on both the 0.940 mm and 2.134 mm perforation samples. The samples were 143 mm long, arranged in the same configuration and loading density as for the stick propellant closed bomb firings. The size of the blowout chamber limited sample lengths to 143 mm. Samples were captured on target cloth stretched in front of the device in such a way as to provide a "soft landing" for the propellant pieces ejected. Most of the grains were recovered intact. Blowout discs were designed to burst at 34.5 MPa. Actual measured burst pressures were 37.4 and 37.9 MPa, respectively, for the experiments with the small and large perforated samples. The ejected grains were subsequently examined microscopically to determine regression distances at the exterior surface and inside the perforation along the length of the grains.

D. Closed Bomb Tests

Closed bomb tests were carried out in the standard BRL 700 cm^3 closed chamber at loading densities at or near 0.25 g/cm^3. Sample weights ranged from 173.0 to 184.7 g, since only whole strands and grains were used. Generally, experiments were run in duplicate with additional samples being run when necessary. Because of the length of the bomb cavity, the maximum sample length was 337 mm. Additional sample lengths appear in Table II. The igniters used in the system consisted of a "mild" electric match (M-100 type) manufactured by the Atlas Company and various weights of black powder. In some cases, the match and a fast granulation black powder (FFFG) were enclosed in a Dacron patch. In others, single perforated black powder pellets were stacked end-to-end, axially aligned with the match and wrapped in cellophane tape. In several tests, DuPont 700X flake double-base propellant was substituted for the black powder ignition aid. All charges were made up in the JANNAF configuration, i.e., propellant sticks and grains stacked and wrapped with cellophane to give a fairly rigid package. The igniter was placed at the center of the charge in some cases and at the end of the charge in others. The packaging procedure was expected to promote good charge ignition. To examine the effects of ignition on extracted burning rate, the ratio of igniter to propellant was varied from 1.7 to 3.5 percent. A series of pictures showing igniter, stick propellant, and an assembled stick propellant charges appear in Figures 3A, 3B, and 3C. Closed bomb data reductions were performed either via the CBRED or BURNX programs.

TABLE II. TEST MATRIX NOSOL 363 PERFORATION AUGMENTED BURNING STUDY

A. Closed Bomb Tests

Propellant	Length mm	Perforation L/D*	Slot	Loading Density**	Igniter
A 336.6	358.1	-	0.25–0.27		BP-FFFG (1.6, 2.5, 2.8, 3.5%)
			BP-Pellet (2.8%)		
			DB-Flake (2.5%)		
A 336.6	---	Yes	0.25	BP-FFFG (3.0%)	
A 167.7	178.4	-	0.25	BP-FFFG (3.0%)	
A 83.8	89.1	-	0.25	BP-FFFG (3.0%)	
A 19.1	20.3	-	0.25	BP-FFFG (3.0%)	
A 19.1	---	Yes	0.25	BP-FFFG (3.0%)	
B 336.6	157.7	-	0.25	BP-FFFG (1.7, 2.5, 3.0, 3.8%)	
			BP-Pellet (3.0%)		
			DB-Flake (2.5%)		
B 336.6	---	Yes	0.25	BP-FFFG (3.0%)	
B 167.7	78.6	-	0.25	BP-FFFG (3.0%)	
B 83.8	39.3	-	0.25	BP-FFFG (3.0%)	
B 19.1	9.0	-	0.25	BP-FFFG (3.0%)	
B 19.1	---	Yes	0.25	BP-FFFG (3.0%)	

B. Interrupted Burning Tests

Propellant	Length mm	Perforation L/D*	Slot	Loading Density**	Igniter
A 142.9	152.0	-	0.20	BP-Pellet (3.4%)	
B 142.9	67.0	-	0.21	BP-Pellet (3.2%)	
B 142.9	---	Yes	0.21	BP-Pellet (3.2%)	

Note: In most cases, runs performed in duplicate, occasionally in triplicate.

* Length-to-diameter ratio

** in g/cm^3

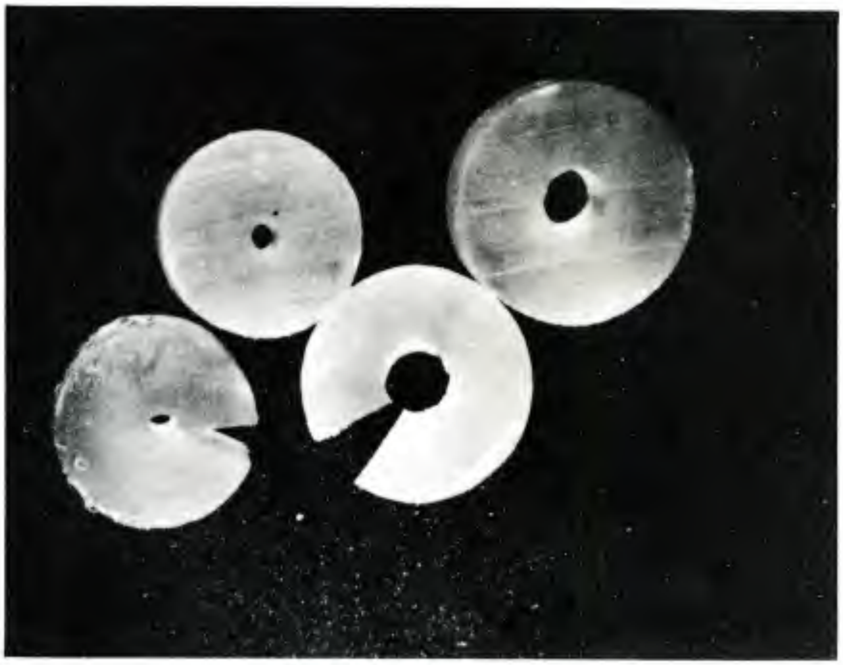

Figure 2. End Views of Slotted and 1P Grains

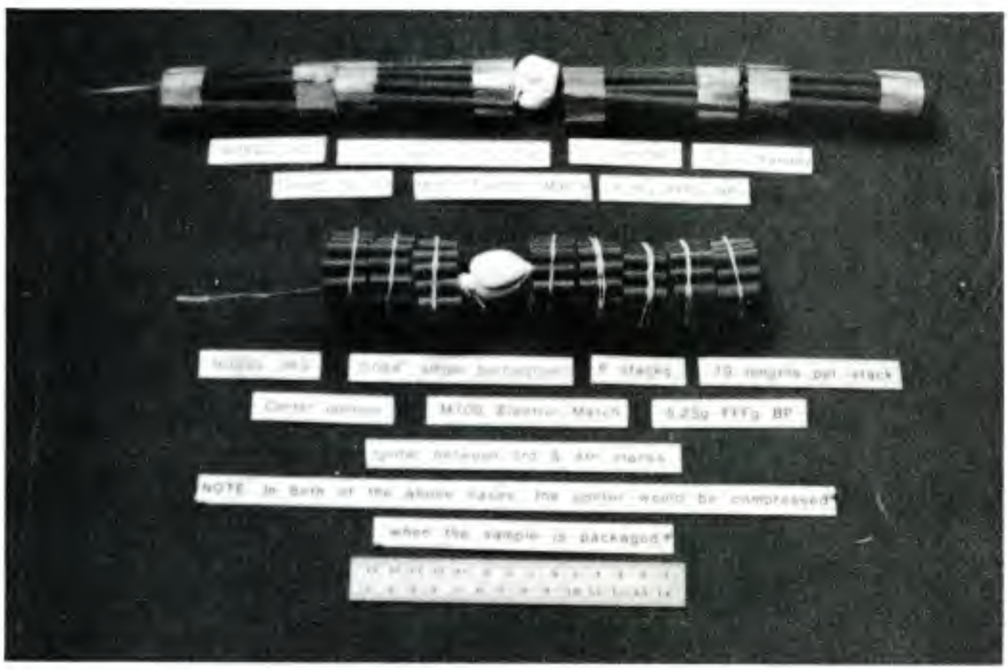

Figure 3A. Granular and Medium Length Stick Charges

Figure 3B. Medium and Long Stick Charges with BP Pellets and FFFG Igniters

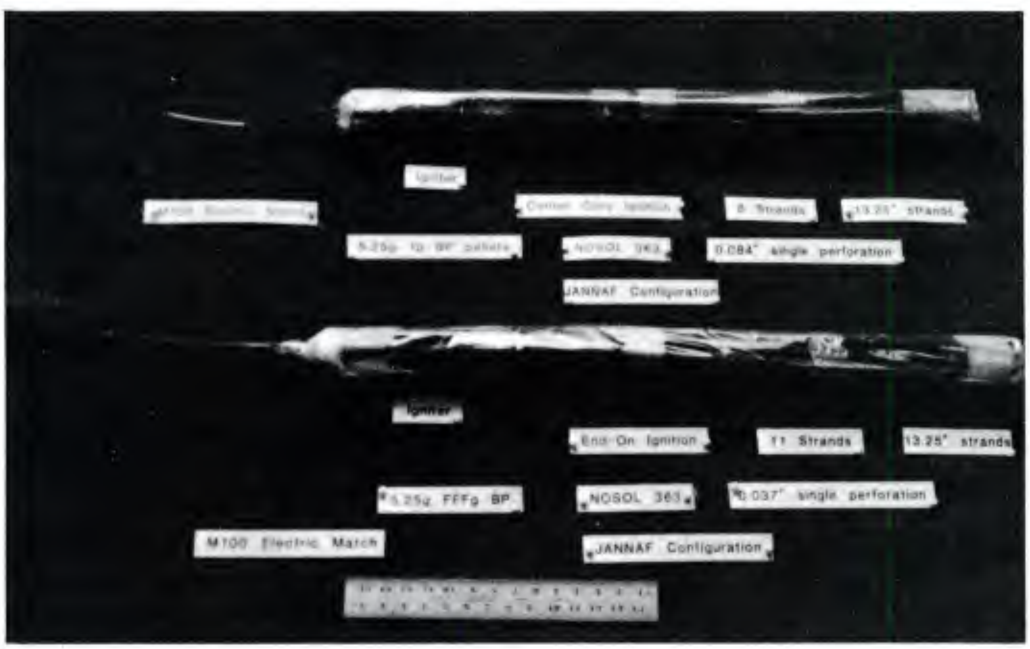

Figure 3C. JANNAF Configuration with Centercore and End-on Ignition

III. RESULTS

A. Reproducibility

The reproducibility of the granular (19 mm long) propellant firings was quite good. An overlay of individual runs for the samples of each perforation diameter (0.940 and 2.134 mm) appears in Figure 4. The burning rates of the

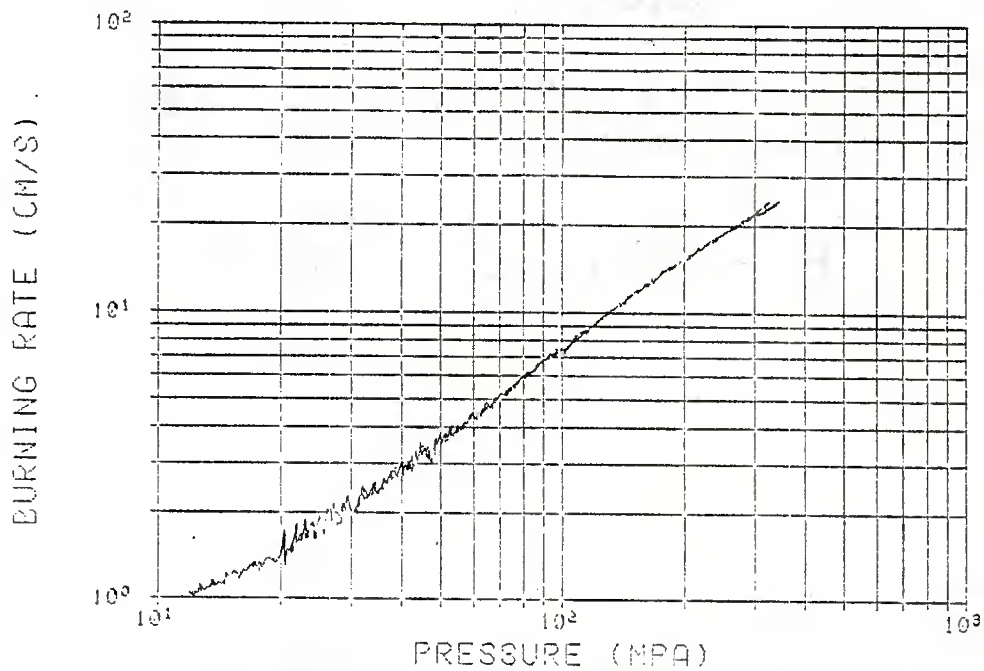

Figure 4. Burning Rate Comparison for 19.1 mm Long, (0.940 and 2.134 mm Perforation Diameter) NOSOL 363 Samples

two samples match with little apparent difference over the 10-300 MPa region. Interestingly, the upper ends of both curves show a decrease in slope above 150 MPa. The round-to-round reproducibility of the slotted propellants was, likewise, excellent. Plots of replicate firings were virtually indistinguishable. The reproducibilities of the burning rate data from the longer (especially the 337 mm long) samples of both perforation diameters, however, were considerably poorer. Superimposed curves from four firings of the 2.134 mm perforation diameter perforated stick samples appear in Figure 5. The increased scatter of the data is evident. Furthermore, a wavy character may be seen on several of the traces, especially in the low pressure region. The wavy character of the burning rate curves is a result of

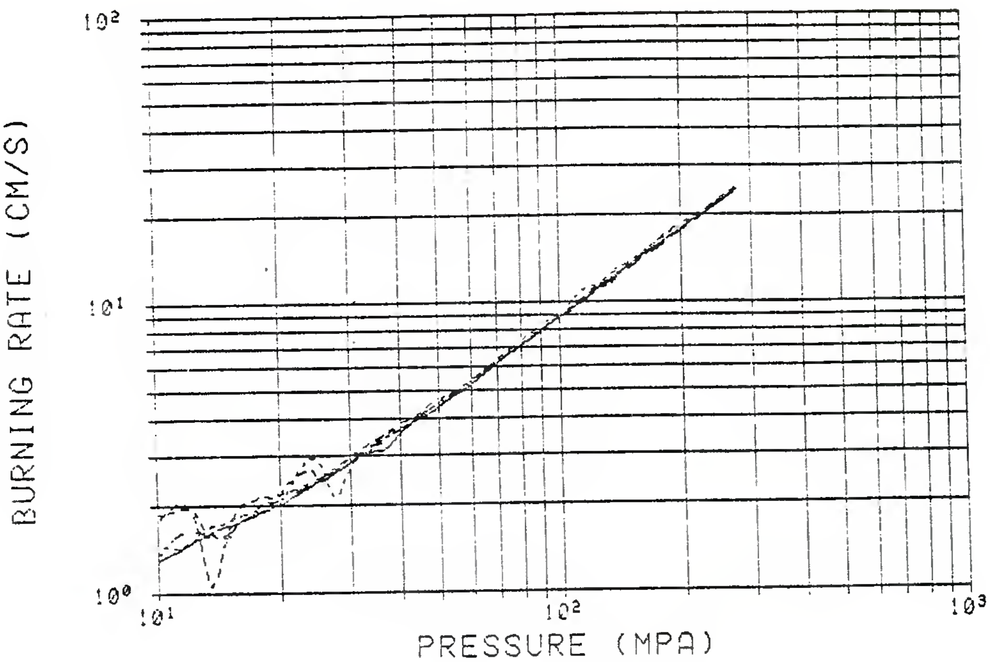

Figure 5. Round-to-Round Reproducibility of 2.134 mm PD, 337 mm Long 1P Stick Propellant Samples

oscillations in the closed bomb, probably excited by the combustion products jetting from the ends of the long single perforated grains. A number of the pressure records contained easily identifiable sinusoidal wave patterns superimposed on the pressure-time trace. A set of reproducibility curves for the smaller, 0.940 mm, perforation diameter stick propellant samples appears in Figure 6. The scatter in the data is, once again, evident, though for these samples there seemed to be fewer chamber oscillations.

B. Form Function Check

The form function subroutines for analyzing the slotted granulation data were written by Mr. F. Lynn, BRL. Since these were new subroutines, it became of interest to independently verify that the same burning rate answers would be given by the single perforated and slotted subroutines under comparable conditions. Accordingly, samples of slotted and single perforated stick propellants from both perforation diameters were cut into 19 mm lengths and fired in the closed bomb. The JANNAF charge configuration was used in both cases. The data were reduced and examined. Figure 7 presents the results

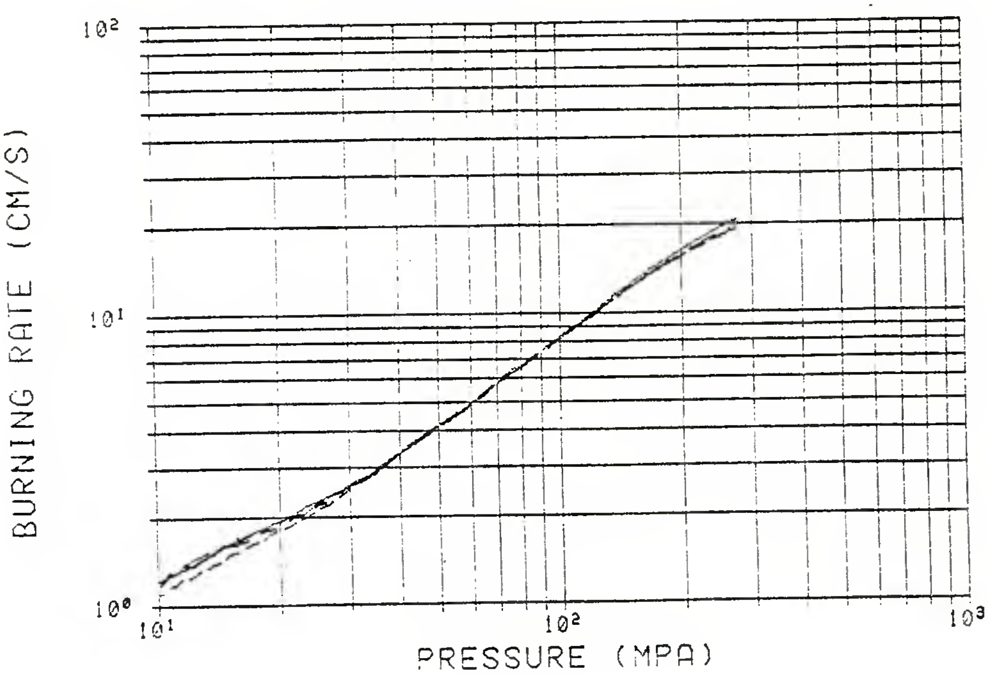

Figure 6. Round-to-Round Reproducibility for 0.940 mm PD, 337 mm Long 1P Stick Propellant Samples

from the short 1P slotted and unslotted granular firings, respectively, for the large perforation diameter samples. The agreement of the data is exceptional. The agreements between analogous firings of the smaller perforation samples was only slightly poorer. As a matter of fact, the agreement between the granular and slotted propellant burning rate data (even for the 337 mm length slotted sticks from both perforation diameter samples) was so good that all these data were subsequently averaged to form the reference data set for comparison with the longer 1P samples.

C. Burning Rates of Larger Perforation Diameter Samples

A comparison of the averaged data from firings of the 2.13 mm perforation diameter samples appears in Figure 8. Included are the data from firings of 337 mm long unslotted and slotted 1P stick samples as well as the unslotted 168 and 19 mm 1P samples. The short (19 mm) and 84 mm long slotted and unslotted 1P samples had virtually identical burning rates. As a matter of fact, even the burning rates of the 168 mm long unslotted 1P samples fall only slightly above the average of the shorter samples. The average burning rates of the 337 mm long 1P samples, however, fall considerably above the rest of the data. The error limits around this curve (cfr. dotted lines) leave little question that there is a significant difference between the burning rates of the unslotted 1P stick samples and the rest.

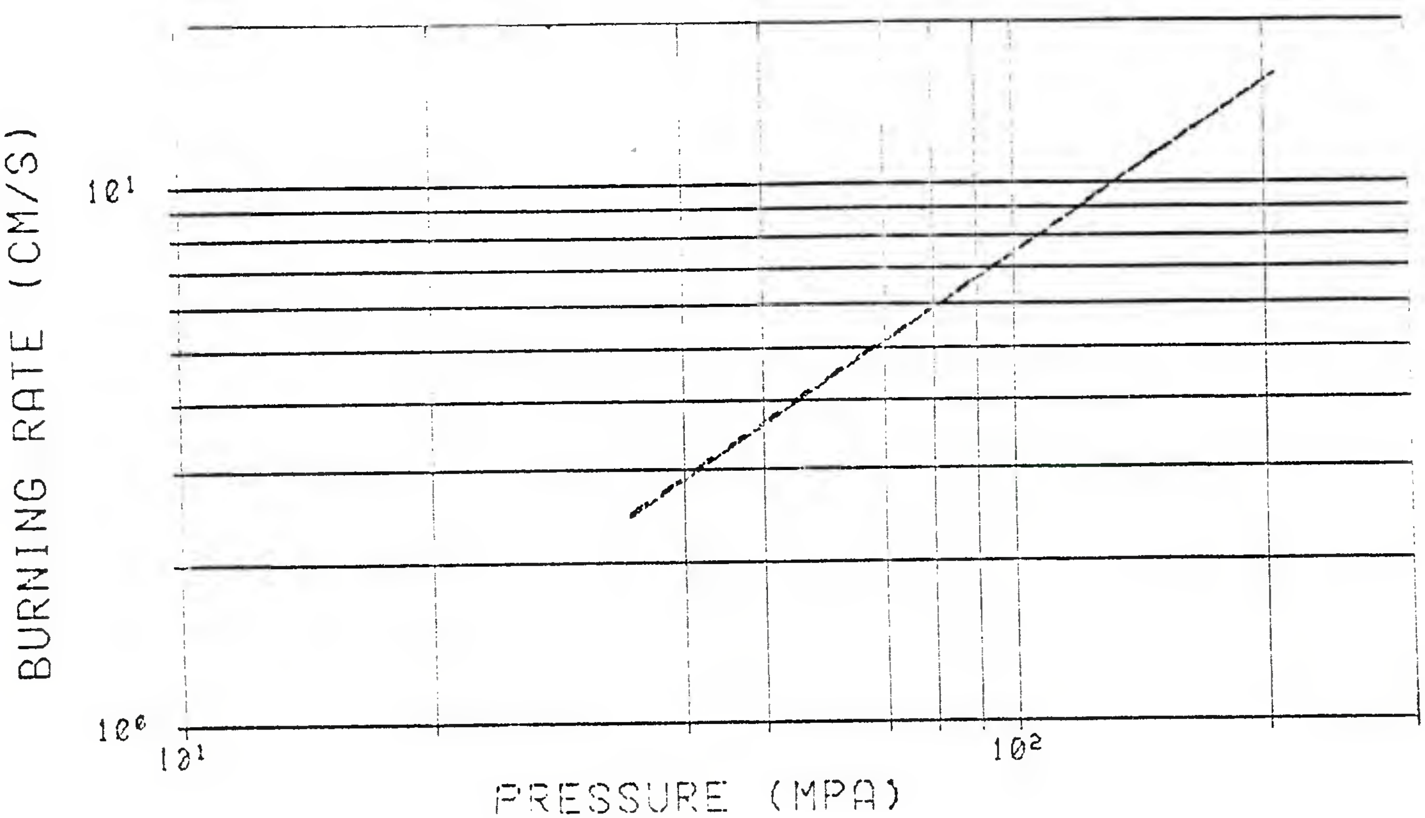

Figure 7. Burning Rate Curves of 2.134 mm PD, 19.1 mm Long 1P and Slotted and Unslotted Samples

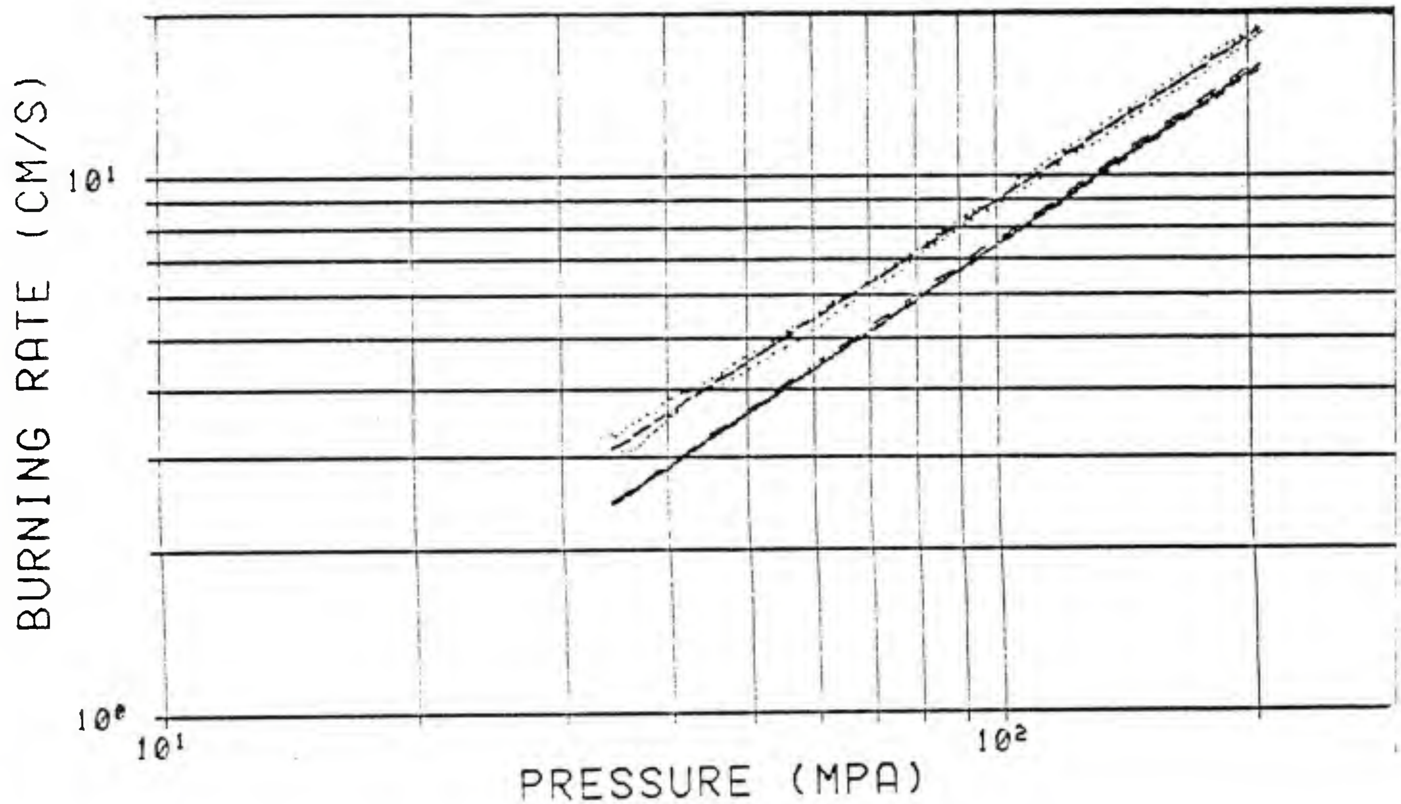

Figure 8. Average Burning Rate Data for 2.134 mm Perforation Family of Samples (Dimensions Indicate Length)

———— 19 mm Slotted and Unslotted 1P Samples
-------- 337 mm Slotted 1P Samples
– – – – 168 mm Unslotted 1P Samples
— — — 337 mm Unslotted 1P Samples

D. Burning Rates of Small Perforation Diameter Samples

The averaged data for various configurations of the 0.940 mm perforation diameter propellant samples appear in Figure 9. As above, the results of the 337 mm single perforated and slotted samples as well as single perforated 168 and 19 mm long samples are included. The slotted and short single perforated granular propellant sample results agree quite closely over the whole pressure range. Unlike above, however, the observed burning rates of the 168 mm long single perforated samples were higher than the rest of the data, including the 337 mm single perforated samples. These results were so unexpected that a considerable amount of energy was expended checking them out. Repetition of the experiments, however, confirmed these findings.

Initially, it appeared that there may have been ignition effects on the extracted burning rates of the long (337 mm) small perforated samples. To check this out, a set of experiments was performed in which the igniters were varied from Bennite strands to black powder pellets to granular (FFFG) black

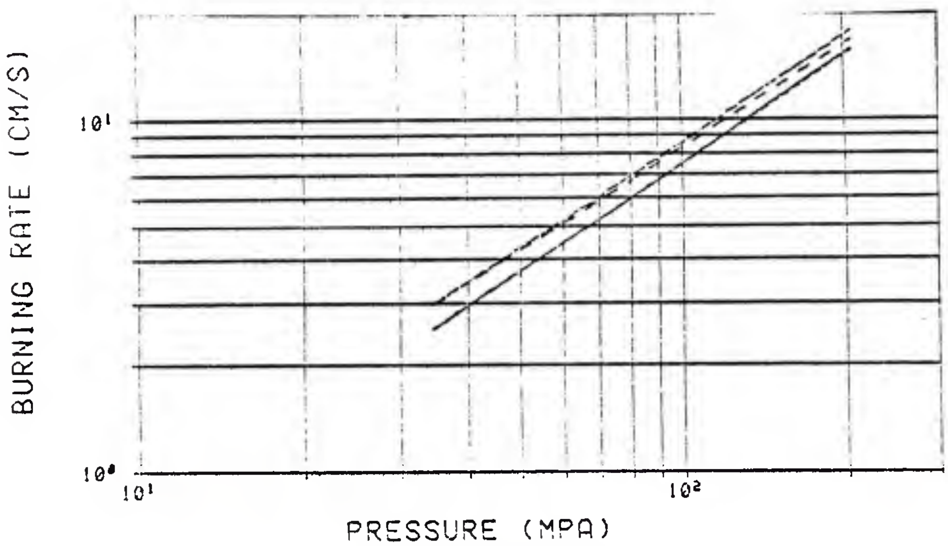

Figure 9. Average Burning Rate Data for 0.940 mm Perforation Family of Samples (Dimensions Indicate Length)

———————— 19 mm Unslotted 1P
- - - - - - - - 337 mm Slotted 1P
— — — 337 mm Unslotted 1P
—— —— —— 168 mm Unslotted 1P

powder. Ultimately, the results could be resolved into a group of ten firings (various igniters and configurations) and two outliers with considerably higher burning rates than the rest of the data. Plots of the data from four "normal" runs and the burning rate curve for one of the outliers are presented in Figure 10. Considering some of the findings to be discussed later, it seems probable that these unusual results were due to drastic grain breakup or splitting during burning.

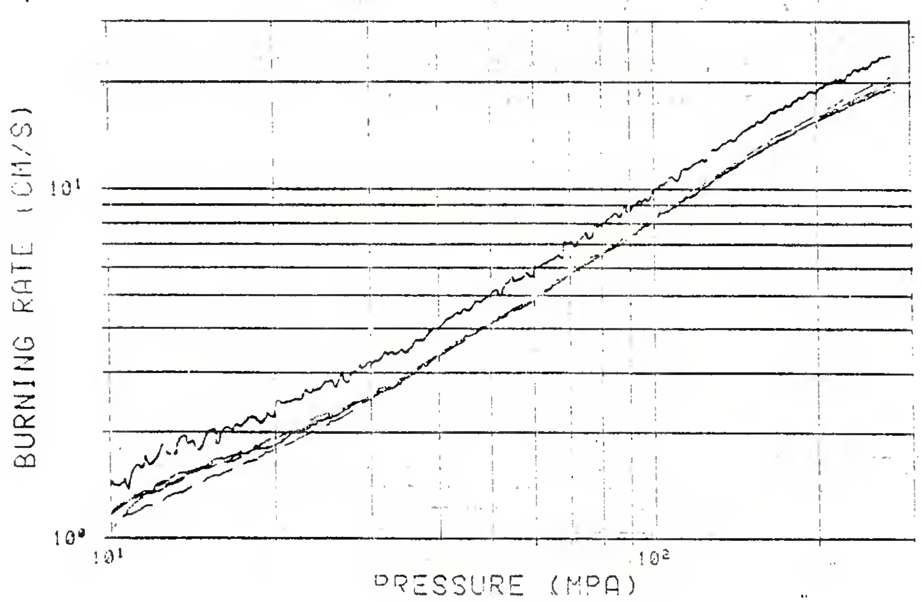

Figure 10. Average Burning Rate Curve and Outlier for 0.940 mm PD, 337 mm Unslotted 1P Stick Propellant

IV. DISCUSSION

A. Mechanistic Considerations

Conventional gun propellants are generally accepted to burn in parallel layers, normal to the sample's surface (Piobert's law). According to this law, burning rates are assumed to depend on pressure and sample chemical composition,(and, tacitly, processing variables) but independent of sample geometry. Under ordinary circumstances, sample geometry and burning rate have

been shown to be independent. A clear cut example of this may be found in a recent JANNAF Round Robin study[10] comparing burning rates of 7 perforated granular and strand propellent samples with identical chemical compositions. The normal gasification process from the surface of a propellant grain is described in Figure 11A. Under certain circumstances, however, the

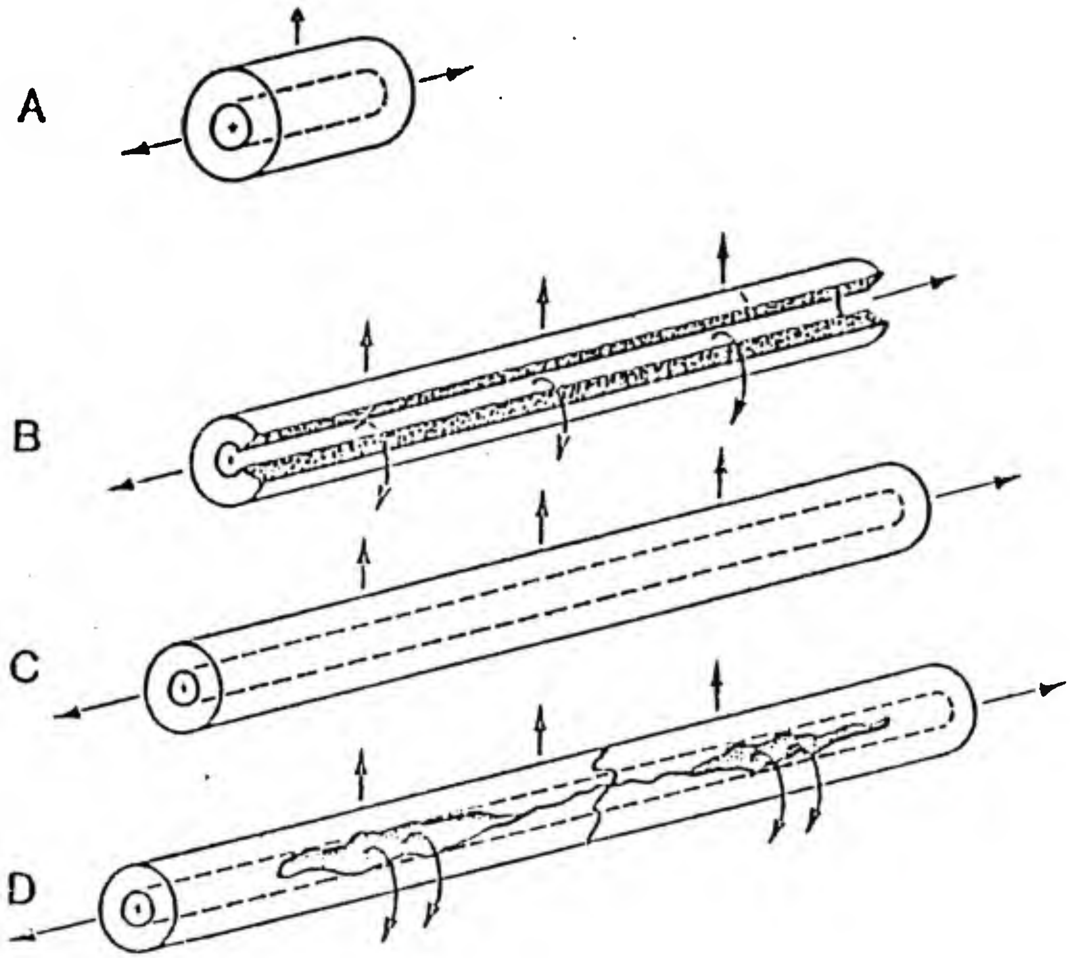

Figure 11. Gas Evolution During Burning of Short Granular and Slotted and Unslotted Stick Propellant

---

[10]*A. Juhasz, ed., "Round Robin Results of the Closed Bomb and Strand Burner," JANNAF Combustion Subcommittee, Burn Rate Measurements and Data Reduction Procedures Panel, CPIA Publication 361, August, 1982.*

assumptions concerning the decoupling of burning rate and sample geometry may collapse. In the case of perforated propellant grains, for instance; provided that the perforation is sufficiently long, conditions may become favorable to allow a coupling between perforation length and burning rate. For example, if the venting of combustion products through the perforation ends is slower than the generation of combustion products within the perforation, a pressure buildup will occur. (See Figure 11C.) The inner surfaces of the grain, therefore, will burn at a higher pressure (and therefore a higher rate) than the outer surfaces. The difference in pressure may also be expected to drive a rapid gas flow through the perforation, setting up conditions favorable for erosive burning. Alternately, if the gas pressure inside the perforation becomes sufficiently high, grain rupture may result, (Figure 11D.) The idea behind the longitudinal slot in slotted stick propellants, is to permit sideways venting of combustion products from inside the perforation, thereby avoiding the perforation pressure buildup and attendant effects. (Figure 11B.)

B. Data Correlations

The close agreement between the burning rates of the short, unslotted single perforated grains and the slotted 337 mm stick samples indicates that slotting does, indeed, serve to eliminate the augmenting influences on propellant burning, at least in the closed bomb. Conversely, the differences between the burning rates of the unslotted single perforated stick and the granular/slotted samples demonstrate clearly that some augmenting mechanisms are operating in the burning of these single-perforated stick samples.

The change in burning rates with sample length appears to follow a regular pattern in the case of the 2.134 mm perforation diameter 1P samples. The greatest augmentation takes place for the longest samples with progressively less augmentation as grain length decreases. This is consistent with both the perforation-pressure-augmented and erosive burning mechanisms. In the case of the 0.940 mm perforation samples, however, the fastest burning rates were not observed for the longest, but for the medium length (168 mm) samples. This is inconsistent with both the mechanisms mentioned above. It seems clear from the results of both sets of samples, however, that up to perforation-length-to-diameter ratios of 40 to 45, augmentation effects are relatively weak. It is interesting also to compare the results of the unslotted 1P stick samples with each other and the reference (averaged granular/slotted) data set. (See Figure 12.) From the curves, it is clear that the greatest overall burning rate augmentation takes place for the large perforation diameter 337 mm long 1P samples

C. Modeling Efforts

(Perforation Pressure Build-up) It became of interest to examine numerically the change in extracted burning rates based on the hypothesis of pressure build-up inside the perforation. To accomplish this, a lumped-parameter interior ballistic code (Baer-Frankle model) was modified to permit the burning rates inside the perforations and on the exterior grain surfaces to be different. The normal $r=AP^n$ burning rate relationship was assumed for both surfaces, however. The pressure inside the perforation was modeled by assuming that the system behaves as a rocket, the gases generated inside the perforation moving to the exterior volume by assuming sonic and subsonic equations of mass flow through the perforation ends. In order to simulate the

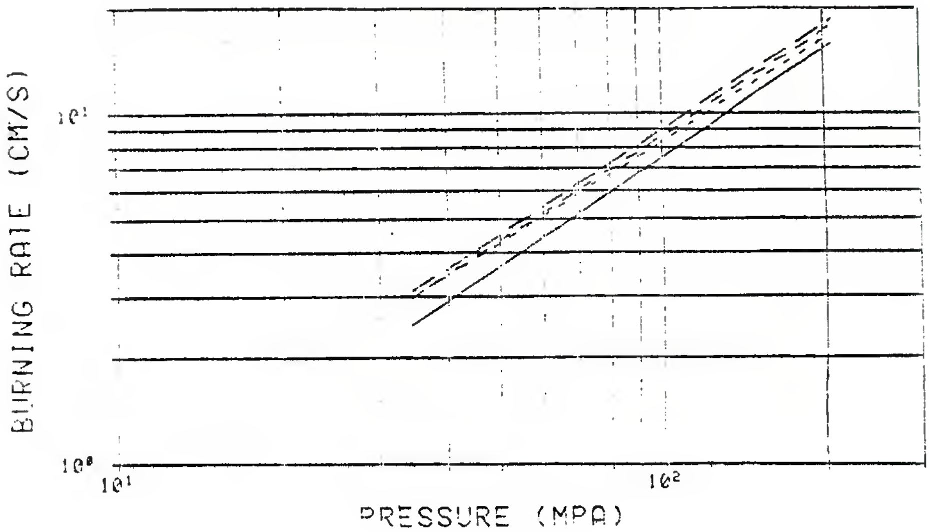

Figure 12. Baseline and Strongly Augmented Burning Rates

——————— 2.134 PD, 337-mm Unslotted 1P sample
— — — 0.940 PD, 168-mm Unslotted 1P sample
---------- 0.940 PD, 337-mm Unslotted 1P sample

closed bomb situation the projectile was not allowed to move (thereby keeping the chamber volume constant). The pressure-time curve so synthesized was then analyzed using a normal closed bomb burning rate reduction code. The closed bomb code assumed identical regression rates for all surfaces.

An increase was noted in the extracted burning rates for both the small- and large-perforated unslotted stick propellant samples.(See Figure 13.) The magnitude of the increase was roughly that of the experimental data, but the order of increase was reversed. According to the perforation-pressure-buildup hypothesis, the effect should be strongest for long grains with small perforation diameters. This is because the volume into which the perforation combustion gases are released is smaller and because the nozzle area through which the gases must exit is smaller. This would lead to higher pressurization and mass generation rates inside the perforation, hence greater extracted apparent burning rates. In actual fact, the single-perforated stick propellant samples with the larger perforation diameters were found to have the higher burning rates.

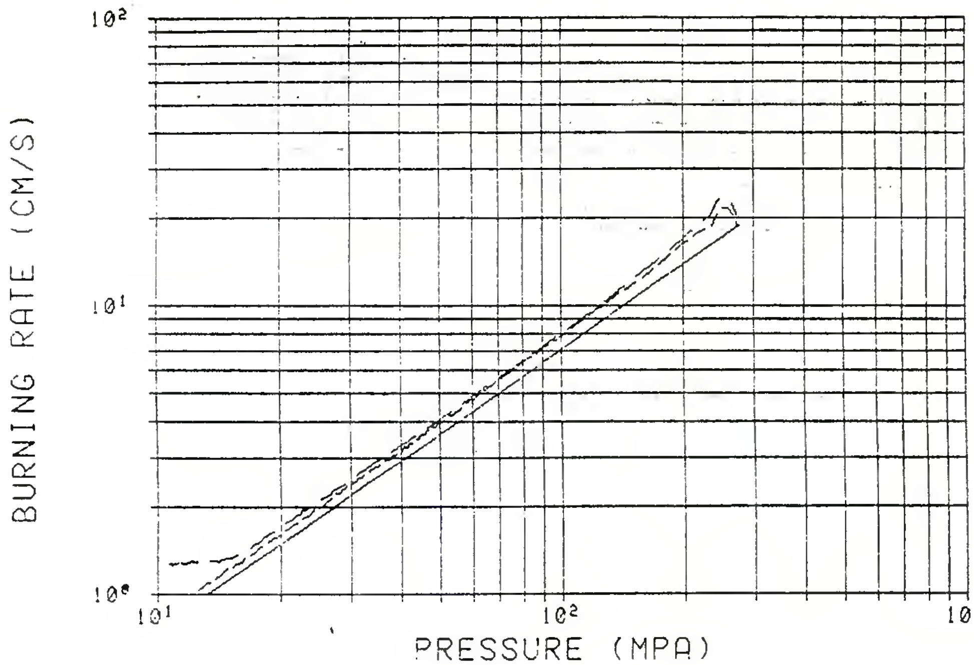

Figure 13. Synthetic Closed Bomb Burning Rate Curves Assuming Perforation Pressure Buildup

——————— Baseline burning rate

- - - - - - - - Prediction for 2.134-mm PD sample

— — — — — Prediction for 0.094-mm PD sample

(Grain Splitting) The pressure differentials calculated between the perforation and the exterior grain surface (above) were greater than rupture pressures previously determined for the samples using static pressurization techniques.[11] Further, the ruptured samples were found to have failed with the formation of longitudinal splits. This prompted numerical examination of the hypothesis of grain splitting during burning. For this portion of the study, a conventional closed bomb synthesis program was modified to allow

---

[11] *F. W. Robbins, "Continuing Study of Stick Propellant Combustion Processes," 19th JANNAF Combustion Meeting, CPIA Publication 366, Vol I, pp 427-442, October 1982.*

changing the assumed surface function from a single-perforated cylinder to a single-perforated cylinder with a slot at some arbitrarily chosen pressure (for the example in Figure 14, the transition was programmed below 10 MPa). In effect, the grain was made to unzip, exposing extra surface area for burning. The resultant synthetic pressure-time curve was analyzed using a normal closed bomb burning rate code as before.

The apparent burning rates extracted from the synthetic curve were higher than the burning rates input to the synthesis program. A plot of the input and extracted data for the 2.134 mm PD sample appears in Figure 14. Interestingly, though the absolute change in burning rates was of the same order as found in our experimental study, little or no difference was found between the apparent burning rates of the small and large perforation diameter samples.

One significant observation from this portion of the study concerns the character of the upper region of the extracted burning rate curve. This

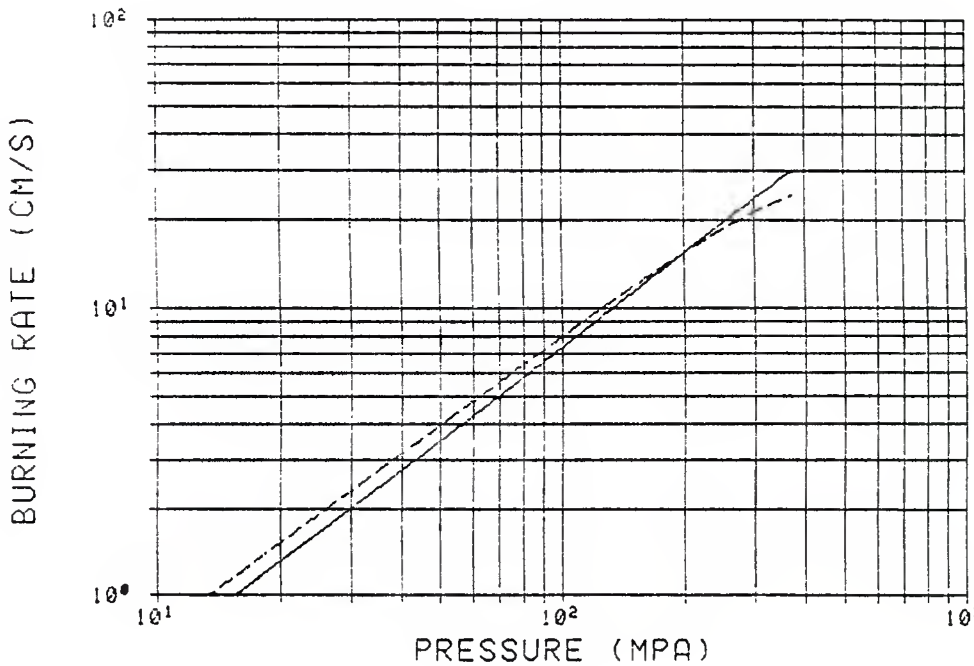

Figure 14. Synthetic Closed Bomb Burning Rate Curves Assuming Grain Splitting
——— Baseline
— — — — Predicted for 2.134 mm PD sample

section of the synthetic curve bears a strong similarity to the upper portion of the experimental data from the 0.940 mm single perforated 1P stick samples of Figure 6. In summary, therefore, although the grain splitting hypothesis can account for an increase in the observed burning rates and for the general shape of the 0.940 mm PD single-perforated stick samples, it fails to account for the observed order of burning rates in the experimental data.

D. Related Observations

Microscopic examination of grains from the interrupted burning tests provides some insight into the way that samples with long perforations burn. For the samples with the small perforation diameters, the distances burned inside the perforation at the two ends of the grain were twice as great as the distances burned on the outer surface. At the center of the grain, however, the perforation distance burned was only two-thirds of the distance burned on the grain exterior. This seems to indicate that there must be a significant, finite time for initial flame propagation through the perforation and that some form of erosive burning augmentation takes place at the perforation ends.

In the case of the samples with large perforation diameter, the distances burned at the grain ends (perforation versus external surface) were roughly the same with possibly a somewhat greater perforation distance burned. At the center of the grain, however, the distance burned inside the perforation was only one half the distance burned at the exterior. This indicates that, for the larger perforation samples, flame propagation into the grain takes longer and that the erosive component of in-perforation burning is considerably less. It should be noted that at the low burst pressures of these experiments ($\sim$ 38 MPa) only 0.1 mass fraction of the propellant would be expected to have burned. It is probable that at higher--or lower--mass fractions burned, the relative distances burned at the various locations may have been different.

In a related study,[11] interrupted burning tests were performed firing stick propellant charges in a sawed-off howitzer. Coning of sample ends (greater regression of the perforation surface than exterior surface), somewhat similar to our results, was noted. In addition, unlike in our study, extensive grain breakup and splitting were also noted.

V. CONCLUSIONS

Overall, it appears that both erosive burning and grain splitting may play significant roles in the burning augmentation of single-perforated stick propellants. The contribution of a simple pressure augmented burning effect in the perforation is more difficult to assess. Considerably more work will be required to dependably establish the relationships between grain length and the various burning augmentation mechanisms. Further interrupted burning tests examining residual grain shapes as a function of mass fraction burned should prove useful in generating a more detailed picture of the process. Closed bomb tests, especially on identical sample lengths as those intended for gun applications are, of course, needed. The experiments with the slotted stick propellant samples indicated essentially identical burning properties as with granular samples. This is interesting in view of observations in gun tests indicating that slotted stick propellants have

higher effective burning rates in guns than the closed bombs. Unlike in the closed bomb, combustion in a gun is accompanied by a rapid movement of product gases past the propellant as projectile motion and gas expansion take place. This may well result in a macroscopic erosive effect, expecially in charges having long, axial channels. It seems likely that combustion studies using a device such as the Dynagun[12] simulator may help to establish the required bridge between stick propellant burning under closed bomb and gun conditions. The Dynagun would permit gross movement of combustion gases across the stick propellant charge in much the same way as they do in a gun. Finally, the picture evolved in this study for the burning of the rather resilient NOSOL 363 stick propellant may not be directly applicable to the highly brittle M30 stick propellant family. Clearly, additional studies of stick propellant burning are needed.

---

[12] *H. Krier and J. W. Black, "Predicting Uniform Gun Interior Ballistics: Part III The Concept and Design of the Dynagun Ballistic Simulator," Technical Report AAE 74-7 U1LU-Eng 74 0507, University of Illinois at Urbana-Champaign, December, 1974.*

ACKNOWLEDGMENTS

The assistance of Mr. Franz Lynn, BRL, for computer support and of Mr. T. C. Smith, NOSIH, who provided the propellant samples used in the study, is gratefully acknowledged.

REFERENCES

1. A. W. Horst and T. C. Minor, "Improved Flow Dynamics in Guns Through the Use of Alternative Propellant Geometries," 1980 JANNAF Propulsion Meeting, CPIA Publication 315, Vol I, pp 325-352, March 1980.

2. T. C. Smith, "Experimental Gun Testing of High Density Multiperforated Stick Propellant Charge Assemblies," 17th JANNAF Combustion Meeting, CPIA Publication 329, Vol II, pp 87-96, November 1980.

3. T. C. Smith and J. A. Kudzall, "Evaluation of Stick Propellant Charge Concepts," 16th JANNAF Combustion Meeting, CPIA Publication 308, Vol I, pp 417-432, December 1979.

4. F. W. Robbins, J. A. Kudzall, J. A. McWilliams, and P. S. Gough, "Experimental Determination of Stick Charge Flow Resistance," 17th JANNAF Combustion Meeting, CPIA Publication 329, Vol II, pp 97-118, November 1980.

5. S. Weiner, "Investigation of Stick Propellant for 155-mm Howitzer, XM198," Interim Memorandum Report, Picatinny Arsenal, July 1975.

6 J. Corner, Theory of the Interior Ballistics of Guns, John Wiley and Sons, NY, 1950.

7. I. W. May and T. C. Minor, "European Trip Report, 18 June - 2 July 1979," Applied Ballistics Branch, Interior Ballistics Division (DRDAR-BLP), Ballistic Research Laboratory, Aberdeen Proving Ground, MD, 1 May 1980.

8. F. W. Robbins and A. W. Horst, "A Single Theoretical Analysis and Experimental Investigation of Burning Processes of Stick Propellant," 18th JANNAF Combustion Meeting, CPIA Publication 347, Vol I, pp 25-34, October 1981.

9. A. Grabowski, S. Weiner and A. J. Beardell, "Closed Bomb Testing of Stick Propellant in Gun Firing Simulation," 17th JANNAF Combustion Meeting, CPIA Publication 329, Vol II, pp 119-124, November 1980.

10. A. Juhasz, ed., "Round Robin Results of the Closed Bomb and Strand Burner," JANNAF Combustion Subcommittee, Burn Rate Measurements and Data Reduction Procedures Panel, CPIA Publication 361, August 1982.

11. F. W. Robbins, "Continuing Study of Stick Propellant Combustion Processes," 19th JANNAF Combustion Meeting, CPIA Publication 366, Vol I, pp 427-442, October 1982.

12. H. Krier and J. W. Black, "Predicting Uniform Gun Interior Ballistics: Part III The Concept and Design of the Dynagun Ballistic Simulator," Technical Report AAE 74-7 UILU-Eng 74 0507, University of Illinois at Urbana-Champaign, December 1974.

DISTRIBUTION LIST

No. Of Copies	Organization
12	Administrator Defense Technical Info Center ATTN: DTIC-DDA Cameron Station Alexandria, VA 22314
1	Office of the Under Secretary of Defense Research & Engineering ATTN: R. Thorkildsen The Pentagon Washington, DC 20301
1	HQDA/SAUS-OR, D. Hardison Washington, DC 20310
1	HQDA/DAMA-ZA Washington, DC 20310
1	HQDA, DAMA-CSM, E. Lippi Washington, DC 20310
1	HQDA/SARDA Washington, DC 20310
1	Commander US Army War College ATTN: Library-FF229 Carlisle Barracks, PA 17013
1	Director US Army Ballistic Missile Defense Advanced Technology Center P. O. Box 1500 Huntsville, AL 35807
1	Chairman DOD Explosives Safety Board Room 856-C Hoffman Bldg. 1 2461 Eisenhower Avenue Alexandria, VA 22331
1	Commander US Army Material Command ATTN: AMRSF-E, Safety Office 5001 Eisenhower Avenue Alexandria, VA 22333
1	Commander US Army Materiel Command ATTN: AMCDRA-ST 5001 Eisenhower Avenue Alexandria, VA 22333
12	Commander US Army Armament R&D Center ATTN: SMCAR-TSS SMCAR-TDC D. Gyorog SMCAR-LCA J. Lannon A. Beardell D. Downs S. Einstein L. Schlosberg S. Westley S. Bernstein P. Kemmey C. Heyman A. Bracuti Dover, NJ 07801
9	Commander US Army Armament R&D Center ATTN: SMCAR-SCA, L. Stiefel B. Brodman SMCAR-LCB-I, D. Spring SMCAR-LCE, R.Walker SMCAR-LCU-CT, E. Barrieres R. Davitt SMCAR-LCU-CV C.Mandala W. Joseph SMCAR-LCM-E, S. Kaplowitz Dover, NJ 07801
1	Commander US Army Material Command ATTN: AMCDE-DW 5001 Eisenhower Avenue Alexandria, VA 22333

DISTRIBUTION LIST

No. Of Copies	Organization
1	Commander US Army Armament R&D Center ATTN: SMCAR-QAR J. Rutkowski Dover, NJ 07801
5	Project Manager Cannon Artillery Weapons System ATTN: AMCPM-CW, F. Menke AMCPM-CWW H. Noble AMCPM-CWS M. Fisette AMCPM-CWA, R. DeKleine H. Hassmann Dover, NJ 07801
2	Project Manager Munitions Production Base Modernization and Expansion ATTN: AMCPM-PMB, A. Siklosi SARPM-PBM-E, L. Laibson Dover, NJ 07801
3	Project Manager Tank Main Armament System ATTN: AMCPM-TMA, K. Russell AMCPM-TMA-105 AMCPM-TMA-120 Dover, NJ 07801
3	Commander US Army Armament R&D Center ATTN: SMCAR LCW-A M.Salsbury SMCAR LCS SMCAR, J. Frasier Dover, NJ 07801
1	Commander US Army Develoment &Employment Agency ATTN: MODE-TED-SAB Fort Lewis, WA 98433
5	Commander US Army Armament Munitions and Chemical Command ATTN: AMSMC-LEP-L, Tech Lib AMSMC-LC, L. Ambrosini AMSMC-IRC, G. Cowan AMSMC-LEM, W. Fortune R. Zastrow Rock Island, IL 61299
1	Commander US Army AMCCOM Benet Weopons Laboratory ATTN: SMCAR-RD, R. Thierry Watervliet, NY 12189
1	Director US Army AMCCOM Benet Weopons Laboratory ATTN: SMCAR-LCB-TL Watervliet, NY 12189
1	Commander US Army Aviation Research and Development Command ATTN: AMSAV -E 4300 Goodfellow Blvd. St. Louis, MO 63120
1	Commander US Army TSARCOM 4300 Goodfellow Blvd. St. Louis, MO 63120
1	Director US Army Air Mobility Research And Development Laboratory Ames Research Center Moffett Field, CA 94035
1	Commander US Army Communications Research and Development Command ATTN: AMSEL-ATDD Fort Monmouth, NJ 07703

DISTRIBUTION LIST

No. Of Copies	Organization
1	Commander US Army Electronics Research and Development Command Technical Support Activity ATTN: AMDSD-L Fort Monmouth, NJ 07703
1	Commander US Army Harry Diamond Lab. ATTN: AMXDO-TI 2800 Powder Mill Road Adelphi, MD 20783
1	Commander US Army Missile Command ATTN: AMSMI-R Redstone Arsenal, AL 35898
1	Commander US Army Natick Research and Development Command ATTN: AMXRE, D. Sieling Natick, MA 01760
1	Commander US Army Tank Automotive Command ATTN: AMSTA-TSL Warren, MI 48090
1	Commander US Army Tank Automotive Command ATTN: AMSTA-CG Warren, MI 48090
1	Project Manager Improved TOW Vehicle ATTN: AMCPM-ITV Warren, MI 48090
2	Program Manager M1 Tank System ATTN: AMCPM-GCM-SA, J. Roossien Warren, MI 48090

No. Of Copies	Organization
1	Project Manager Fighting Vehicle Systems ATTN: DRCPM-FVS Warren, MI 48090
1	Director US Army TRADOC Systems Analysis Activity ATTN: ATAA-SL, White Sands Missile Range, NM 88002
1	Project Manager M-60 Tank Development ATTN: DRCPM-M60TD Warren, MI 48090
1	Commander US Army Training & Doctrine Command ATTN: ATCD-MA/ MAJ Williams Fort Monroe, VA 23651
2	Commander US Army Materials and Mechanics Research Center ATTN: AMXMR-ATL Tech Library Watertown, MA 02172
1	Commander US Army Research Office ATTN: Tech Library P. O. Box 12211 Research Triangle Park, NC 27709
1	Commander US Army Mobility Equipment Research & Development Command ATTN: AMDME-WC Fort Belvoir, VA 22060
1	Commander US Army Logistics Mgmt Ctr Defense Logistics Studies Fort Lee, VA 23801

DISTRIBUTION LIST

No. Of Copies	Organization
1	Commandant US Army Infantry School ATTN: ATSH-CD-CSO-OR Fort Benning, GA 31905
1	US Army Armor & Engineer Board ATTN: STEBB-AD-S Fort Knox, KY 40121
1	Commandant US Army Aviation School ATTN: Aviation Agency Fort Rucker, AL 36360
1	Commandant US Army Command and General Staff College Fort Leavenworth, KS 66027
1	Commandant US Army Special Warfare School ATTN: Rev & Tng Lit Div Fort Bragg, NC 28307
1	Commandant US Army Engineer School Ft. Belvoir, VA 22060
1	Commander US Army Foreign Science & Technology Center ATTN: DRXST-MC-3 220 Seventh Street, NE Charlottesville, VA 22901
1	President US Army Artillery Board Ft. Sill, OK 73503
2	Commandant US Army Field Artillery School ATTN: ATSF-CO-MW, B. Willis Ft. Sill, OK 73503

No. Of Copies	Organization
3	Commandant US Army Armor School ATTN: ATZK-CD-MS/ M. Falkovitch Armor Agency Fort Knox, KY 40121
1	Chief of Naval Materiel Department of the Navy ATTN: J. Amlie Washington, DC 20360
1	Office of Naval Research ATTN: Code 473, R. S. Miller 800 N. Quincy Street Arlington, VA 22217
1	Commander Naval Sea Systems Command ATTN: SEA-62R2, R. Beauregard National Center, Bldg. 2 Room 6E08 Washington, DC 20360
1	Commander Naval Air Systems Command ATTN: NAIR-954-Tech Lib Washington, DC 20360
1	Strategic Systems Project Office Dept. of the Navy Room 901 ATTN: J. F. Kincaid Washington, DC 20376
1	Assistant Secretary of the Navy (R, E, and S) ATTN: R. Reichenbach Room 5E787 Pentagon Bldg. Washington, DC 20350
1	Commander Naval Research Lab Tech Library Washington, DC 20375

DISTRIBUTION LIST

No. Of Copies	Organization
5	Commander Naval Surface Weapons Center ATTN: Code G33, J. L. East W. Burrell J. Johndrow Code G23, D. McClure Code DX-21 Tech Lib Dahlgren, VA 22448
2	Commander US Naval Surface Weapons Center ATTN: J. P. Consaga C. Gotzmer Indian Head, MD 20640
4	Commander Naval Surface Weapons Center ATTN: S. Jacobs/Code 240 Code 730 K. Kim/Code R-13 R. Bernecker Silver Spring, MD 20910
2	Commanding Officer Naval Underwater Systems Center Energy Conversion Dept. ATTN: CODE 5B331, R. S. Lazar Tech Lib Newport, RI 02840
4	Commander Naval Weapons Center ATTN: Code 388, R. L. Derr C. F. Price T. Boggs Info. Sci. Div. China Lake, CA 93555
2	Superintendent Naval Postgraduate School Dept. of Mechanical Engineering ATTN: A. E. Fuhs Code 1424 Library Monterey, CA 93940
6	Commander Naval Ordnance Station ATTN: P. L. Stang J. Birkett S. Mitchell C. Christensen D. Brooks Tech Library Indian Head, MD 20640
1	AFSC/SDOA Andrews AFB, MD 20334
1	Program Manager AFOSR Directorate of Aerospace Sciences ATTN: L. H. Caveny Bolling AFB, DC 20332
6	AFRPL (DYSC) ATTN: D. George J. N. Levine B. Goshgarian D. Thrasher N. Vander Hyde Tech Library Edwards AFB, CA 93523
1	AFFTC ATTN: SSD-Tech LIb Edwards AFB, CA 93523
1	AFATL/DLYV Eglin AFB, FL 32542
1	AFATL/DLXP ATTN: W. Dittrich Eglin AFB, FL 32542
1	AFATA/DLD ATTN: D. Davis Eglin AFB, FL 32542
1	AFATL/DLDL ATTN: O. K. Heiney Eglin AFB, FL 32542

DISTRIBUTION LIST

No. Of Copies	Organization
1	AFATL/DLODL ATTN: Tech Lib Eglin AFB, FL 32542
1	AFFDL ATTN: TST-Lib Wright-Patterson AFB, OH 45433
1	Lawrence Livermore Laboratory ATTN: M. S. L-355, M. Finger P. O. Box 808 Livermore, CA 94550
1	NASA/Lyndon B. Johnson Space Center ATTN: NHS-22, Library Section Houston, TX 77058
1	Aerodyne Research, Inc. Bedford Research Park ATTN: V. Yousefian Bedford, MA 01730
1	Aerojet Solid Propulsion Co. ATTN: P. Micheli Sacramento, CA 95813
1	Atlantic Research Corporation ATTN: M. K. King 5390 Cheorokee Avenue Alexandria, VA 22314
1	AVCO Everett Rsch Lab ATTN: D. Stickler 2385 Revere Beach Parkway Everett, MA 02149
2	Calspan Corporation ATTN: C. Morphy P. O. Box 400 Buffalo, NY 14225
1	Foster Miller Associates ATTN: A. Erickson 135 Second Avenue Waltham, MA 02154

No. Of Copies	Organization
1	Commander US Army Missile Command AMSMI-YDL Redstone Arsenal, AL 35890
1	General Applied Sciences Lab ATTN: J. Erdos Merrick & Stewart Avenues Westbury Long Island, NY 11590
1	General Electric Company Armament Systems Dept. ATTN: M. J. Bulman, Room 1311 Lakeside Avenue Burlington, VT 05401
1	Hercules, Inc. Allegany Ballistics Laboratory ATTN: R. B. Miller P. O. Box 210 Cumberland, MD 21501
1	Hercules, Inc Bacchus Works ATTN: K. P. McCarty P. O. Box 98 Magna, UT 84044
1	Hercules, Inc. Eglin Operations AFATL DLDL ATTN: R. L. Simmons Eglin AFB, FL 32542
1	IITRI ATTN: M. J. Klein 10 W. 35th Street Chicago, IL 60616
1	Lawrence Livermore Laboratory ATTN: M. S. L-355, A. Buckingham P.O. Box 808 Livermore, CA 94550

DISTRIBUTION LIST

No. Of Copies	Organization
1	Olin Corporation Badger Army Ammunition Plant ATTN: R. J. Thiede Baraboo, WI 53913
1	Olin Corporation Smokeless Powder Operations ATTN: R. L. Cook P. O. Box 222 St. Marks, FL 32355
1	Paul Gough Associates, Inc. ATTN: P. S. Gough P. O. Box 1614 Portsmouth, NH 03801
1	Physics International Company 2700 Merced Street San Leandro, CA 94577
1	Princeton Combustion Research Lab., Inc. 4751 US Highway One Monmouth Junction, NJ 08852
1	Pulsepower Systems, Inc. ATTN: L. C. Elmore 815 American Street San Carlos, CA 94070
2	Rockwell International Rocketdyne Division ATTN: BA08 J. E. Flanagan J. Gray 6633 Canoga Avenue Canoga Park, CA 91304
1	Science Applications, Inc. ATTN: R. B. Edelman 23146 Cumorah Crest Woodland Hills, CA 91364
1	Scientific Research Assoc., Inc. ATTN: H. McDonald P. O. Box 498 Glastonbury, CT 06033
3	Thiokol Corporation Huntsville Division ATTN: D. Flanigan R. Glick Tech Library Huntsville, AL 35807
2	Thiokol Corporation Wasatch Division ATTN: J. Peterson Tech Library P. O. Box 524 Brigham City, UT 84302
2	Thiokol Corporation Elkton Division ATTN: R. Biddle Tech Lib. P. O. Box 241 Elkton, MD 21921
2	United Technologies Chemical Systems Division ATTN: R. Brown Tech Library P. O. Box 358 Sunnyvale, CA 94086
1	Universal Propulsion Company ATTN: H. J. McSpadden Black Canyon Stage 1 Box 1140 Phoenix, AZ 85029
1	Veritay Technology, Inc. ATTN: E. B. Fisher Propulsion Department 4845 Millersport Highway P. O. Box 305 East Amherst, NY 14051

DISTRIBUTION LIST

No. Of Copies	Organization
1	Southwest Research Institute Institute Scientists 8500 Cubebra Road San Antonio, TX 78228
1	Battelle Memorial Institute ATTN: Tech Library 505 King Avenue Columbus, OH 43201
1	Brigham Young University Dept. of Chemical Engineering ATTN: M. Beckstead Provo, UT 84601
1	California Institute of Tech 204 Karman Lab Main Stop 301-46 ATTN: F. E. C. Culick 1201 E. California Street Pasadena, CA 91125
1	Director Jet Propulsion Laboratory ATTN: L. D. Strand 4800 Oak Grove Drive Pasadena, CA 91109
1	University of Illinois AAE Department ATTN: H. Krier Transportation Bldg. Rm 105 Urbana, IL 61801
1	University of Massachusetts Dept. of Mechanical Engineering ATTN: K. Jakus Amherst, MA 01002
1	University of Minnesota Dept. of Mechanical Engineering ATTN: E. Fletcher Minneapolis, MN 55455

No. of Copies	Organization
1	Case Western Reserve University Division of Aerospace Sciences ATTN: J. Tien Cleveland, OH 44135
3	Georgia Institute of Tech School of Aerospace Eng. ATTN: B. T. Zinn E. Price W. C. Strahle Atlanta, GA 30332
1	Institute of Gas Technology ATTN: D. Gidaspow 3424 S. State Street Chicago, IL 60616
1	Johns Hopkins University Applied Physics Laboratory Chemical Proplsion Information Agency ATTN: T. Christian Johns Hopkins Road Laurel, MD 20707
1	Massachusetts Institute of Technology Dept of Mechanical Engineering ATTN: T. Toong Cambridge, MA 02139
1	Pennsylvania State University Applied Research Lab ATTN: G. M. Faeth P. O. Box 30 State College, PA 16801
1	Pennsylvania State University Dept. Of Mechanical Engineering ATTN: K. Kuo University Park, PA 16802

DISTRIBUTION LIST

No. Of Copies	Organization
1	Purdue University School of Mechanical Engineering ATTN: J. R. Osborn TSPC Chaffee Hall West Lafayette, IN 47906
1	Rensselaer Polytechnic Inst. Department of Mathematics Troy, NY 12181
1	Rutgers University Dept. of Mechanical and Aerospace Engineering ATTN: S. Temkin University Heights Campus New Brunswick, NJ 08903
1	SRI International Propulsion Sciences Division ATTN: Tech Library 333 Ravenswood Avenue Menlo Park, CA 94025
1	Stevens Institute of Technology Davidson Laboratory ATTN: R. McAlevy, III Hoboken, NJ 07030
2	Director Los Alamos Scientific Lab ATTN: T3, D. Butler M. Division, B. Craig P. O. Box 1663 Los Alamos, NM 87544
1	University of Southern California Mechanical Engineering Dept. ATTN: OHE200, M. Gerstein Los Angeles, CA 90007
2	University of Utah Dept. of Chemical Engineering ATTN: A. Baer G. Flandro Salt Lake City, UT 84112

No. Of Copies	Organization
1	University of Princeton AMES Department ATTN: F. Williams Princeton, NJ 08540
1	Washington State University Dept. of Mechanical Engineering ATTN: C. T. Crowe Pullman, WA 99163
1	AFWL/SUL Kirtland AFB, NM 87117
1	Teledyne McCormick Selph ATTN: C. Leveritt 3601 Union Road Hollister, CA 95023

Aberdeen Proving Ground

Dir, USAMSAA
ATTN: AMXSY-D
AMXSY-MP, H. Cohen
Cdr, USATECOM
ATTN: AMSTE-TO-F
STECS-MT, S. Walton
G. Rice
D. Lacey
C. Herud
Dir, HEL
ATTN: J. Weisz
Cdr, CRDC, AMCCOM
ATTN: SMCCR-RSP-A
SMCCR-MU
SMCCR-SPS-IL

USER EVALUATION SHEET/CHANGE OF ADDRESS

This Laboratory undertakes a continuing effort to improve the quality of the reports it publishes. Your comments/answers to the items/questions below will aid us in our efforts.

1. BRL Report Number ________________ Date of Report ________

2. Date Report Received ________________

3. Does this report satisfy a need? (Comment on purpose, related project, or other area of interest for which the report will be used.) ________

4. How specifically, is the report being used? (Information source, design data, procedure, source of ideas, etc.) ________

5. Has the information in this report led to any quantitative savings as far as man-hours or dollars saved, operating costs avoided or efficiencies achieved, etc? If so, please elaborate. ________

6. General Comments. What do you think should be changed to improve future reports? (Indicate changes to organization, technical content, format, etc.)

CURRENT ADDRESS

Name

Organization

Address

City, State, Zip

7. If indicating a Change of Address or Address Correction, please provide the New or Correct Address in Block 6 above and the Old or Incorrect address below.

OLD ADDRESS

Name

Organization

Address

City, State, Zip

(Remove this sheet along the perforation, fold as indicated, staple or tape closed, and mail.)